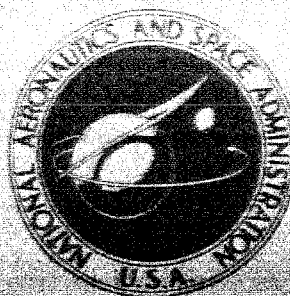


NASA TECHNICAL
MEMORANDUM



NASA TM X-1100

NASA TM X-1100

N65-26250	
ACCESSION NUMBER	DATE
24	1
PAGES	CODE
	C3
NASA OR GPO OFFICE NUMBER	CATEGORY

GPO PRICE \$ _____
CFSTI
GTS PRICE(S) \$ 1.00

Hard copy (HC) _____

Microfilm (MF) 51

OPERATING STABILITY OF THE APOLLO FUEL-CELL CONDENSER

by Michael B. Weinstein

Lewis Research Center

Cleveland, Ohio

OPERATING STABILITY OF THE APOLLO FUEL-CELL CONDENSER

By Michael B. Weinstein

**Lewis Research Center
Cleveland, Ohio**

NATIONAL AERONAUTICS AND SPACE ADMINISTRATION

For sale by the Clearinghouse for Federal Scientific and Technical Information
Springfield, Virginia 22151 - Price \$1.00

OPERATING STABILITY OF THE APOLLO FUEL-CELL CONDENSER

by Michael B. Weinstein

Lewis Research Center

SUMMARY

An experimental evaluation of the Apollo fuel-cell condenser conducted at the Lewis Research Center showed that there are no operating instabilities in the small condensing tubes.

Motion pictures taken of the condensate emerging from the condensing passages coupled with traces of the fluctuations in the pressure differential across the condenser show that the condensate flow in the tubes is controlled by surface tension and viscous forces, and that operation in zero gravity should not alter the condenser's operation.

INTRODUCTION

The Apollo fuel-cell condenser is intended to remove both the water and waste heat produced by the fuel cell. The condenser is to operate over a wide range of inlet conditions in a zero-gravity environment.

In order to determine if there were any condensing instabilities in the small condensing tubes, or if the mode of condensation was such that instabilities might occur in zero-gravity operation, a ground test evaluation was conducted at the Lewis Research Center.

The condenser removes the product water by condensing it from a recirculating hydrogen and water-vapor stream. It transfers the excess heat from this gas stream to a glycol-water solution which in turn passes through a radiator.

Photographs of the condenser (figs. 1 to 3) show the small trapezoidal flow passages in which the condensation takes place and the placement of the coolant and gas stream inlet and outlet passages. Drawings of the condenser (figs. 4 and 5) show the internal placement of the flow passages. The condenser has been designed to condense 0.8 pound per hour of water under the following conditions:

Hydrogen flow, lb/hr	5.0
Water vapor flow, lb/hr	11.4
Condensate, lb/hr	0.8
Coolant flow, lb/hr	80
Gas inlet temperature, °F	253
Gas outlet temperature, °F	200
Coolant inlet temperature, °F	181
Coolant outlet temperature, °F	211
Operating pressure, psia	60

Under the most unfavorable conditions specified, the condensing rate was 2.34 pounds per hour. This condition occurs when the fuel cell is operating at maximum power output (2200 W).

SYMBOLS

- A orifice area, sq in.
- C_w orifice coefficient
- H_s specific humidity, (lb H₂O)/(lb H₂)
- K gas constant, (lb mass)(°R)/(lb force)(sec)
- P pressure upstream of orifice, psia
- T temperature, °R
- t time, sec
- \dot{w} gas flow rate, lb/hr
- Y coolant flow rate, lb/hr

APPARATUS AND PROCEDURE

A test rig designed for extensive control of all important condenser operating parameters (inlet temperatures, gas and coolant flow rates, and operating pressures) was assembled (fig. 6). Special gas inlet and outlet headers were fabricated for the condenser to facilitate the measurement of pertinent gas parameters while allowing the photographing of the two-phase flow at the condenser exit (figs. 7 and 8).

The parameters under operator control were the following:

- (1) Hydrogen flow rate before mixing
- (2) Steam flow rate before mixing
- (3) Gas inlet temperature to the condenser
- (4) Gas pressure at the condenser exit
- (5) Coolant flow rate
- (6) Coolant inlet temperature

The measured parameters were the following:

- (1) Gas outlet temperature
- (2) Water condensation rate
- (3) Pressure differential ΔP across the condensing tubes
- (4) Coolant outlet temperature

The manner in which these parameters were measured and controlled will now be discussed.

The flow rates of the hydrogen and water vapor streams were controlled by controlling the temperatures and pressures at the respective choked orifices. These orifices (fig. 9) were calibrated (flow rate as a function of upstream pressure and temperature) by using either nitrogen or helium. From these calibrations the orifice areas were calculated from the choked orifice equation

$$\dot{w} = \frac{3600 P A C_w K}{T^{1/2}}$$

where C_w was assumed equal to 0.83. The flow rates of hydrogen and water vapor were calculated from these areas and the respective constants (K) for each gas. The temperatures and pressures upstream of the orifices were measured with Chromel-Alumel thermocouples and Bourdon gages, respectively. In this manner the temperatures and pressures were read to precisions of $\pm 1^\circ \text{F}$ and $\pm 0.5 \text{ psia}$.

The operating pressures were measured and recorded as follows: The gas pressure at the condenser outlet header was measured with a 10-inch, 100-psig Heise gage and also was recorded on an 'XYY' plotter by using the electrical output from a pressure transducer.

The pressure differential ΔP across the condensing tubes was measured with a 0.15-psid transducer that was calibrated at least once a week and zero checked prior to every run.

All temperatures were measured with Chromel-Alumel thermocouples referenced to 32°F and read from a digital voltmeter.

Some difficulty was encountered in obtaining accurate readings of the condenser outlet temperature. The water ejected from the condensing tubes was found to be striking the thermocouple probe (fig. 7(a)) and causing lower than expected readings. To im-

prove this situation a liquid drop deflector made of plastic tubing was placed over the thermocouple.

The flow rate of the glycol-water solution used as the coolant was batch measured by using a 1000-milliliter volumetric flask and a stopwatch. The time periods needed to fill the flask, measured to 0.1 second, were used to calculate the flow rate.

DATA REDUCTION - ERROR ANALYSIS

The calculations made when using the experimental data were as follows:

- (1) Hydrogen and steam flow rates through the choked orifices
- (2) Inlet humidity to the condenser
- (3) Coolant flow rates

Gas Flow Rates

Since there are errors inherent in the method used to measure or calculate the values of all the terms in the choked orifice flow equation

$$\dot{w} = \frac{3600 \text{ PAC}_w K}{T^{1/2}} \quad (1)$$

there are possible errors in the calculated values of \dot{w} . A maximum value for the error in \dot{w} can be found by differentiating equation (1) and adding all terms:

$$\begin{aligned} d\dot{w} = & \frac{3600 \text{ PAC}_w dK}{T^{1/2}} + \frac{3600 \text{ PAK } dC_w}{T^{1/2}} + \frac{3600 \text{ PC}_w K dA}{T^{1/2}} \\ & + \frac{3600 \text{ AC}_w K dP}{T^{1/2}} + \frac{3600 \frac{1}{2} \text{ PAC}_w dT}{T^{3/2}} \end{aligned} \quad (2)$$

where $d\dot{w}$ is related to the errors in all the other quantities (dP , dT , etc.).

To obtain an idea of the magnitudes of $d\dot{w}$ for both steam and hydrogen, sample data points are utilized as follows:

For steam:

$$\begin{array}{ll} P = 142 \text{ psia} & dP = \pm 0.5 \text{ psia} \\ T = 809^\circ \text{ R} & dT = \pm 2^\circ \text{ R} \\ C_w = 0.83 & dC_w = 0 \quad (C_w \equiv 0.83) \\ A = 1.95 \times 10^{-3} \text{ sq in.} & dA = 1 \times 10^{-5} \text{ sq in.} \\ K = 0.412 & dK = 1 \times 10^{-3} \end{array}$$

When direct substitution is made in equations (1) and (2),

$$d\dot{w} = 0.16 \text{ lb/hr}$$

$$\dot{w} = 12.0 \text{ lb/hr}$$

and

$$100 \frac{d\dot{w}}{\dot{w}} = 1.3 \text{ percent maximum}$$

For hydrogen:

$$\begin{array}{ll} P = 168 \text{ psia} & dP = \pm 0.5 \text{ psia} \\ T = 501^\circ \text{ R} & dT = \pm 2^\circ \text{ R} \\ A = 1.91 \times 10^{-3} \text{ sq in.} & dA = 1 \times 10^{-5} \text{ sq in.} \\ K = 0.1402 & dK = 0.2 \times 10^{-3} \\ C_w = 0.83 & dC_w = 0 \end{array}$$

When direct substitution is made with hydrogen data values,

$$100 \frac{d\dot{w}}{\dot{w}} = 1.3 \text{ percent maximum}$$

The condenser inlet humidity

$$H_s = \frac{\dot{w}_{H_2O}}{\dot{w}_{H_2}} \quad (3)$$

when differentiated is

$$dH_s = \frac{\dot{w}_{H_2} (d\dot{w}_{H_2O}) - \dot{w}_{H_2O} (d\dot{w}_{H_2})}{(\dot{w}_{H_2})^2}$$

Direct substitution of the previous flow rates yields

$$dH_s = 0.07$$

$$H_s = 2.0$$

and

$$100 \frac{dH_s}{H_s} = 4 \text{ percent maximum}$$

For all data points the following are assumed:

$$100 \frac{d\dot{w}_{H_2O}}{\dot{w}_{H_2O}} = 1.3 \text{ percent}$$

$$100 \frac{d\dot{w}_{H_2}}{\dot{w}_{H_2}} = 1.3 \text{ percent}$$

$$100 \frac{dH_s}{H_s} = 4 \text{ percent}$$

It is noted that all possible errors are maximized. The flow rate (lb/hr) of coolant is directly related to the time needed (in sec) to fill a 1000-milliliter volumetric flask. When a density of 1.026 grams per cubic centimeter is used for a solution of 70 weight percent glycol in water,¹

¹Extrapolated from data for a 62.5 percent solution at 200° F found in reference 1.

$$Y(\text{lb/hr}) \text{ of coolant} = 0.123 Y(\text{cc/sec})$$

$$Y(\text{lb/hr}) \cong \frac{10\,000}{1.23 Y} \frac{\text{sec}}{1000 \text{ cc}} = t(\text{sec})$$

$$Y = \frac{8120}{t} \quad (4)$$

Now from equation (4),

$$dY = \frac{8120}{t^2} dt$$

for

$$t = 100 \text{ sec}$$

$$dt = 0.1 \text{ sec}$$

$$dY = 0.08 \cong 0.1 \text{ lb/hr}$$

Therefore a maximum error in Y of 0.2 pound per hour is assumed.

RESULTS AND DISCUSSION

Traces of the gage pressure at the condenser exit header and the ΔP across the condenser as functions of time were recorded on an 'XYY' plotter (samples, fig. 10).

From these traces it is evident that the overall fluctuations in ΔP are a small percentage of the full ΔP values; however, individual tube fluctuations may be larger than those shown on the plots, since the taps for the ΔP transducer are in the large volume headers at each end.

Another fact indicated by both the data (table I) and the ΔP traces is that the average ΔP is fairly constant (0.06 psi) over all the runs. The differences shown in table I (0.05 to 0.07 psi) do not seem to be related to any changes in operating conditions.

A number of tests at condensing rates above the Apollo mission maximum (2.34 lb/hr) showed that even under these conditions operation was stable (fig. 10(b), table I).

Motion pictures of the condensate emerging from the condensing tubes at three condensate rates (0.96, 1.06, and 3.06 lb/hr) were taken at normal (24 fps) and high (240 fps) camera speeds.

TABLE I. - CONDENSER DATA

Date	Run time, min	Steam			Hydrogen			Humidity, lb/lb	Condenser				Flask fill time, sec	Coolant			Condensate removal rate, lb/hr	
		Orifice pressure, psia	Orifice temperature, °R	Orifice area, sq in.	Flow rate, lb/hr	Orifice pressure, psia	Orifice temperature, °R		Orifice area, sq in.	Flow rate, lb/hr	Inlet temperature, °F	Outlet temperature, °F		Pressure, psig	Pressure differential, ΔP, psia	Inlet temperature, °F		Flow rate, lb/hr
(a)																		
1/31	30	151	986	1.98×10^{-3}	11.50 ± 0.15	141	503	1.91×10^{-3}	5.02 ± 0.06	2.29 ± 0.09	251	203	45.0	(b)	80.4	185	211	0.96
2/4	38	144	937	1.95×10^{-3}	11.30 ± 0.15	140	492	1.91×10^{-3}	5.03 ± 0.06	2.25 ± 0.09	226	201	45.0	0.06	80.8	183	207	1.23
	45	140	945	1.95	10.95 ± 0.14	139.5	497	1.91	5.00 ± 0.06	2.19 ± 0.09	226	199	45.0	.06	79.2	184	207	1.12
	30	148	985	1.95	11.32 ± 0.15	168.5	498	1.91	6.04 ± 0.08	1.88 ± 0.08	222	192	45.0	.06	78.8	182	204	.80
2/6	61	142	923	1.98×10^{-3}	11.21 ± 0.15	168	501	1.91×10^{-3}	6.01 ± 0.08	1.87 ± 0.08	287	195	45.0	----	78.0	185	212	0.63
3/3	41	136	870	1.98×10^{-3}	11.05 ± 0.14	177	519	1.23×10^{-3}	4.10 ± 0.05	2.70 ± 0.11	226	---	45.0	0.06	80.4	182.5	201.5	1.34
	30	136	870	1.95	11.05 ± 0.14	177	522	1.23	4.10 ± 0.05	2.70 ± 0.11	225	---	45.0	.06	81.5	186	201.5	1.14
3/5	60	136	810	1.98×10^{-3}	11.47 ± 0.15	174	480	1.23×10^{-3}	6.10 ± 0.05	2.80 ± 0.11	248	---	45.0	0.05	78.5	185	210	1.12
3/6	15	148.5	846	1.98×10^{-3}	12.25 ± 0.16	140	504	1.91×10^{-3}	4.98 ± 0.06	2.46 ± 0.10	346	---	45.0	0.05	180	185	217.5	3.31
							508		4.97 ± 0.06	2.46 ± 0.10	374	---	.05	180	185	221	3.21	
							508		4.97 ± 0.06	2.46 ± 0.10	406	---	.05	178	181.5	224	3.26	
							510		4.96 ± 0.06	2.47 ± 0.10	432	---	.06	178	178.5	222.5	3.44	
						141	510		4.96 ± 0.06	2.47 ± 0.10	470	---	.06	178	179	231	3.28	
3/16	15	164	906	1.95×10^{-3}	13.10 ± 0.17	173	524	1.91×10^{-3}	6.04 ± 0.08	2.17 ± 0.09	310	---	45.0	0.07	203	182	208	2.41
			903	1.95	13.10 ± 0.17	173	524	1.91	6.04 ± 0.08	2.17 ± 0.09	442	---	.07	203	182	225	2.20	
3/17	15	138	882	1.95×10^{-3}	11.10 ± 0.14	167	499	1.91×10^{-3}	5.97 ± 0.08	1.86 ± 0.08	225	---	45.0	0.06	81.2	186	204.5	1.06
		163.5	917	1.95	12.93 ± 0.17	173.5	502	1.23	4.00 ± 0.05	3.24 ± 0.13	370	---	.06	180	180	216	3.05	

a 1964.

b Uncalibrated ΔP.

c Photographs of run made; data inconsistent.

These movies show that the condensate does not "flow" out of the tubes as it is formed, but collects in each tube until it is ejected as a slug or a stream of drops. The movies show that this mode of operation is common to all of the 260 condensing tubes, and also that the only difference caused by an increase in condensing rate is that more slugs per unit time are ejected.

A sequence of frames taken from one of the films is reproduced in figure 11. These frames, covering a time period of 1/10 second, show a condensate slug emerging from a tube.

This condensing mode is consistent with the traces of ΔP against time. The movies show that at any given time some tubes are filling with condensate and a smaller number of tubes are ejecting. The ejecting process accounts for the momentary ΔP increases, and the averaging out of the condensate ejecting into the header from the 260 tubes accounts for the very stable mean ΔP .

In order to show that surface tension forces, acting on the condensate in the tubes, do predominate over those of gravity when the condenser operates in a horizontal position, an experiment to measure the surface tension head in the tube was performed.

A degreased condenser was held in the vertical position over a water bath so that the tube exits were at the surface of the water. Then the gas pressure needed to force the water out of a tube was measured (fig. 12).

The distribution plate at the gas inlet end of the condenser was removed in order to apply gas pressure to single tubes. Gas pressure was built up by letting water drip slowly into a closed vessel, and the gas was introduced into single tubes through a hypodermic needle. The gas pressure was then read from an inclined water manometer when a bubble was seen emerging from a tube exit.

In this experiment, the gas pressures needed to blow the water out were measured for 45 tubes (table II). The average gas pressure was found to be 1.65 centimeters of water with most of the points falling between 1.55 and 1.75 centimeters (36 of 45).

This value of 1.65 centimeters is very close to that which can be calculated for a trapezoidal tube assuming perfect wetting (contact angle, 0°) and an effective radius:

$$h = \frac{2\gamma}{rdg}$$

where

h head, cm of water

γ surface tension, dynes/cm

r effective radius of tube, $(A/\pi)^{1/2}$, cm

d density of water, gm/cc

g 980 cm/sec^2

TABLE II. - MEASURED VALUES OF GAS PRESSURE NEEDED
TO FORCE LIQUID OUT OF A SINGLE TUBE

Tube	^a Pressure, cm of water	Tube	^a Pressure, cm of water	Tube	^a Pressure, cm of water
1	1.33	16	1.70	31	1.75
2	1.25	17	1.60	32	1.59
3	1.60	18	1.79	33	1.65
4	1.37	19	1.56	34	1.79
5	1.66	20	1.70	35	1.78
6	1.62	21	1.69	36	1.55
7	1.65	22	1.59	37	1.65
8	1.68	23	1.71	38	1.62
9	1.68	24	1.68	39	1.65
10	1.65	25	1.68	40	1.73
11	1.60	26	1.67	41	1.85
12	1.50	27	1.71	42	1.60
13	1.67	28	1.62	43	1.68
14	1.68	29	1.65	44	1.80
15	1.72	30	1.74	45	1.75

^aAverage pressure, 1.65 centimeters of water.

The area of one tube is approximately 2.34×10^{-2} square centimeter (fig. 5), and the radius of a circle having this area is 0.062 centimeter. Consequently,

$$h = 1.94 \text{ cm of water}$$

when

$$d = 1.00 \text{ gm/cc}$$

$$g = 980 \text{ cm/sec}^2$$

$$\gamma = 59 \text{ dynes/cm at } 200^\circ \text{ F}$$

Since one tube is only about 0.07 inch high (0.18 cm), gravitational forces would not be expected to have much of an effect on the condensate behavior in a tube.

On the basis of the data presented and a study of the condensing pictures, it can be stated that the surface tension and dynamic pressure differential forces acting on the condensate in the tubes are prime factors controlling condensate removal.

The liquid condensate is held in a tube by surface tension forces acting on the tube interior and at the tube exit. When sufficient pressure head is built up to overcome these forces the slug is blown free.

Since the controlling force during one-gravity operation (tubes horizontal) is surface tension, rather than gravity, it is evident that under zero-gravity conditions the surface tension effect will be predominant.

CONCLUSIONS

1. With the condenser operating horizontally in a one-gravity environment, there is no evidence of any operating instability over a wide range of condensate rates.
2. Small differences in the tube to tube condensing modes are averaged out by the large number of tubes to give very stable operation.
3. Since the surface tension rather than gravity forces control the condensate removal mechanism, no problem areas are envisioned in zero-gravity operation.

Lewis Research Center,
National Aeronautics and Space Administration,
Cleveland, Ohio, February 12, 1965.

REFERENCE

1. Geankoplis, C. J.; Kay, W. B.; Lemmon, A. W.; and Robinson, W.: Heat-Transfer Fluids for Aircraft-Equipment Cooling Systems. TR 54-66, WADC, Feb. 1954.

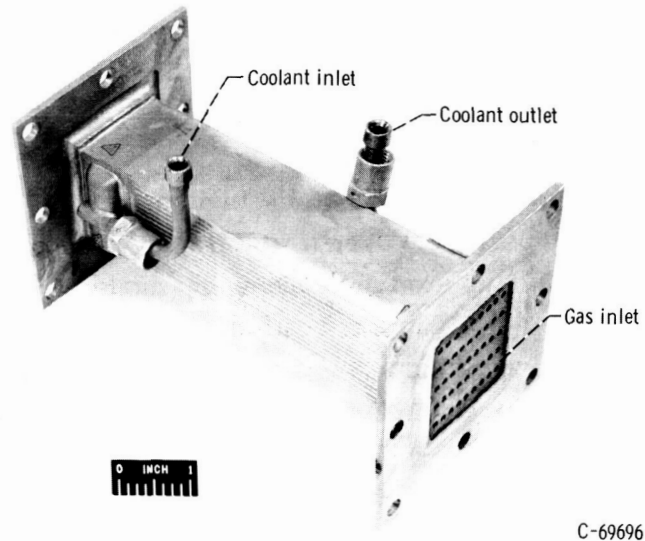


Figure 1. - Apollo fuel-cell condenser.

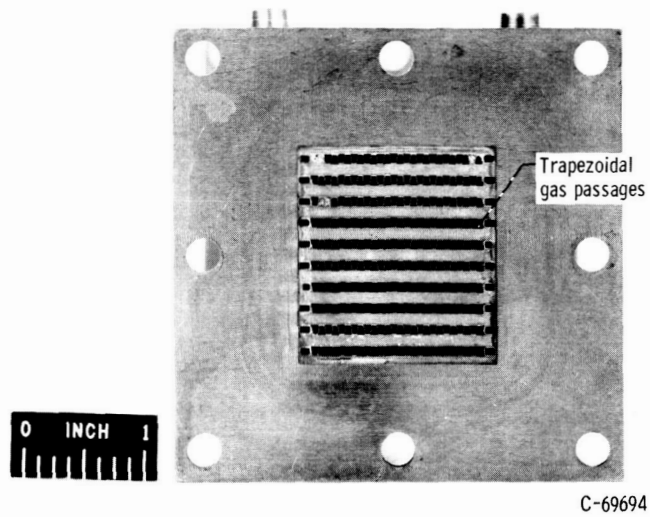


Figure 2. - Condenser exit.

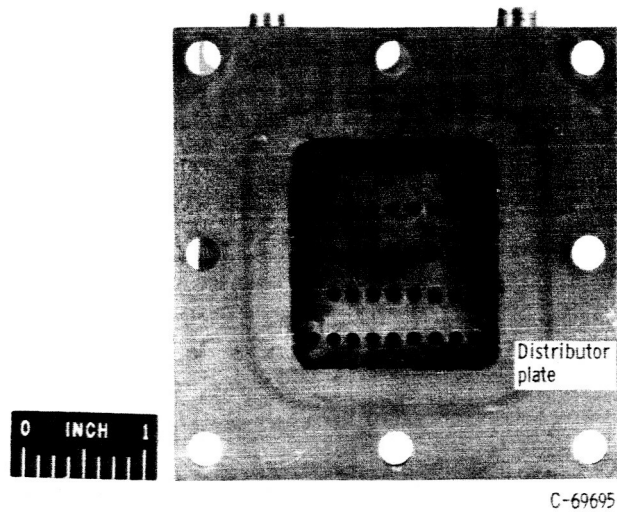


Figure 3. - Condenser gas inlet.

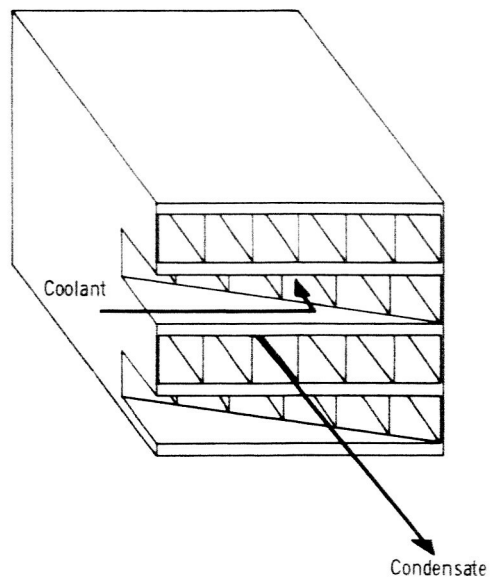


Figure 4. - Condensing and coolant passages.

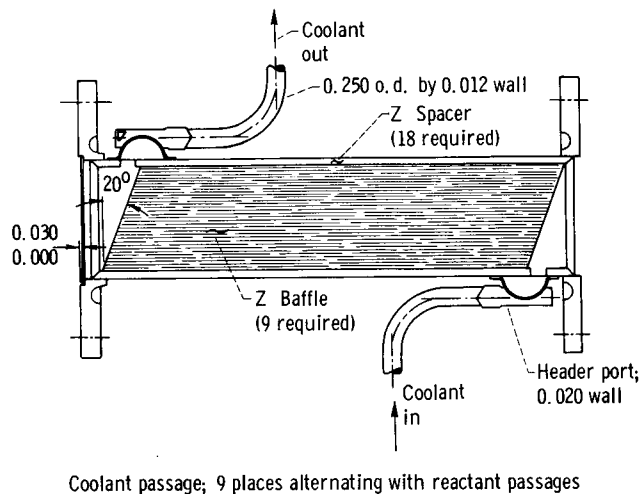
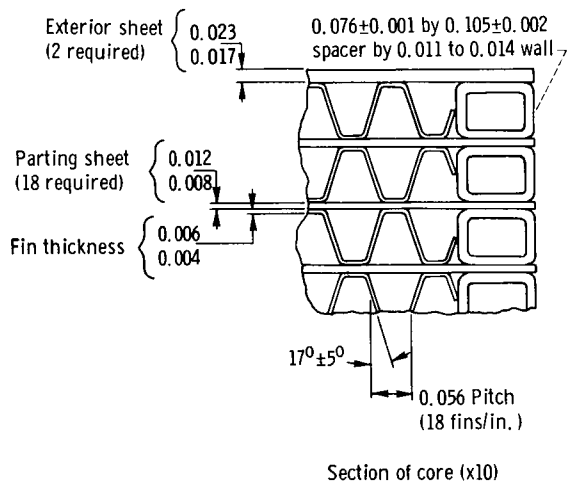


Figure 5. - Condenser. (All dimensions in inches.)

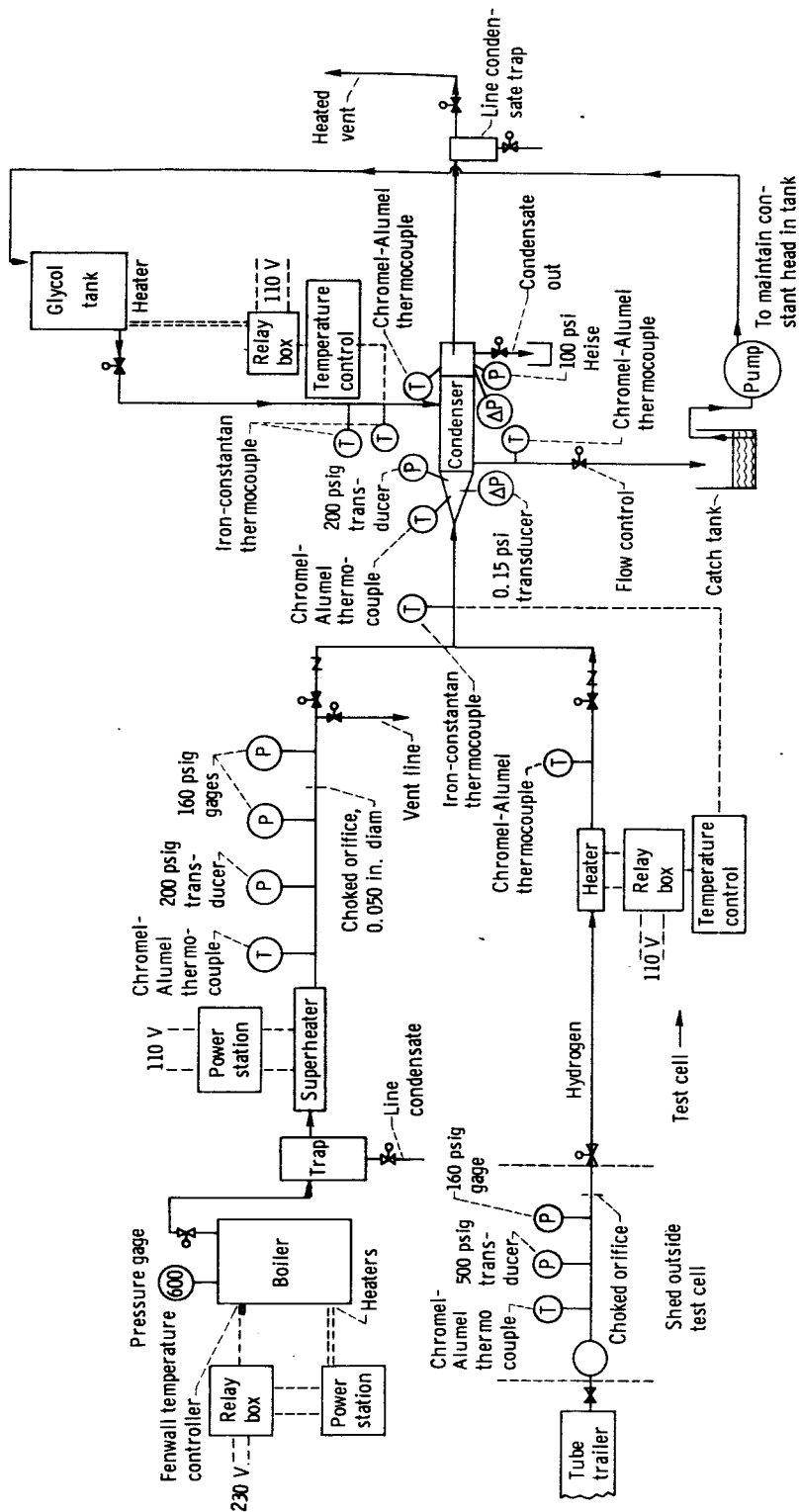
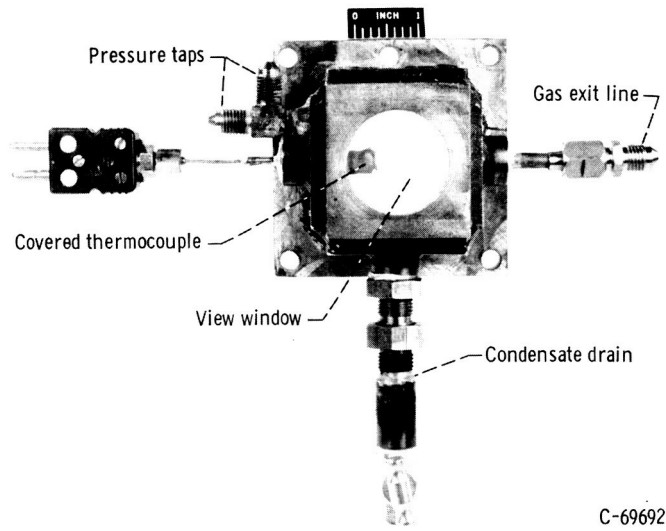
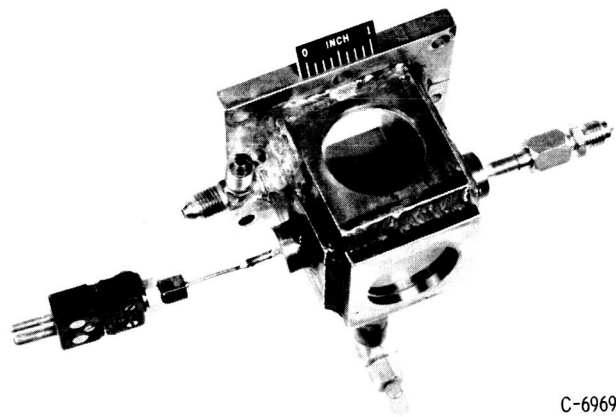


Figure 6. - Flow diagram for condenser experiment.



C-69692

(a) Back view.



C-69690

(b) Top view.
Figure 7. - Exit header.

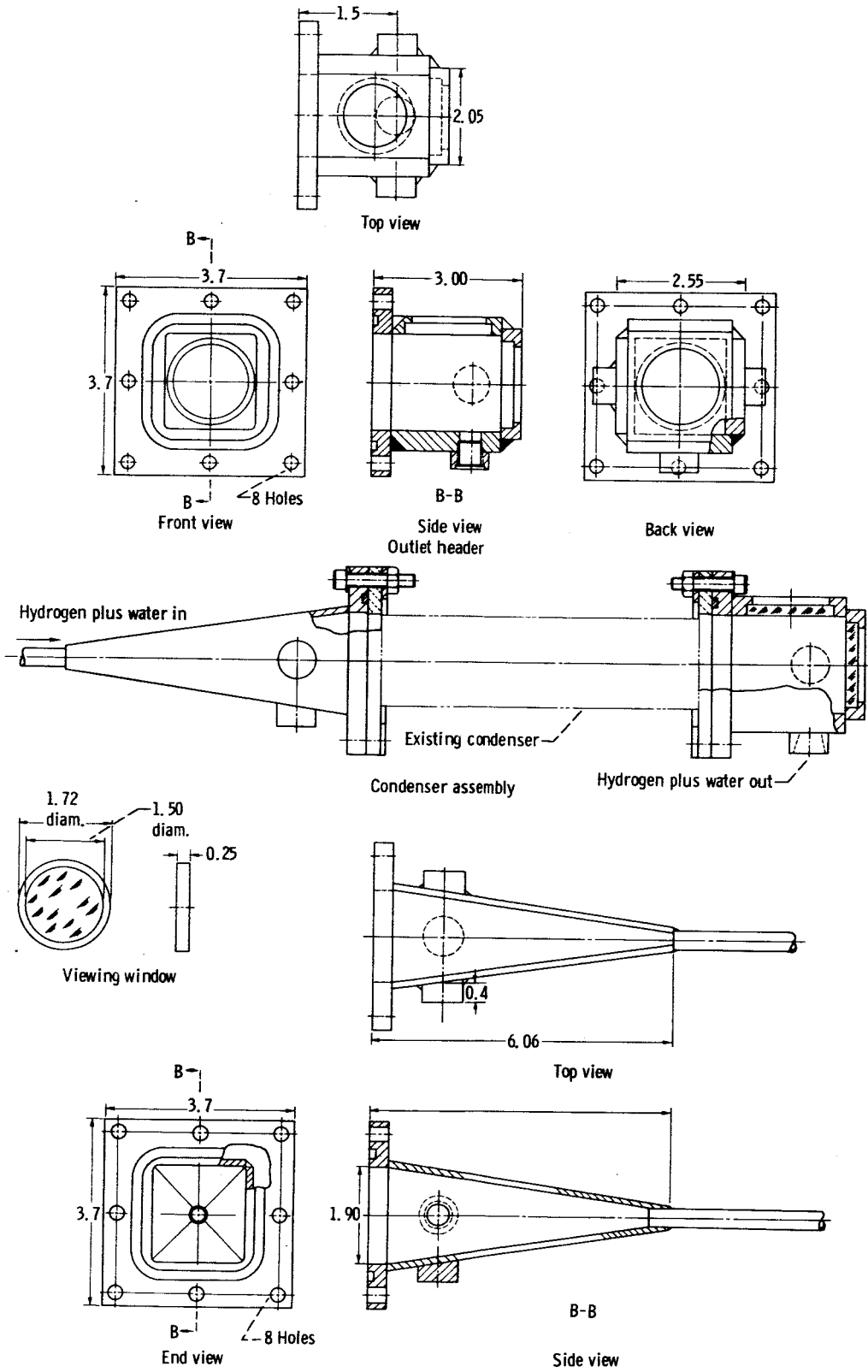
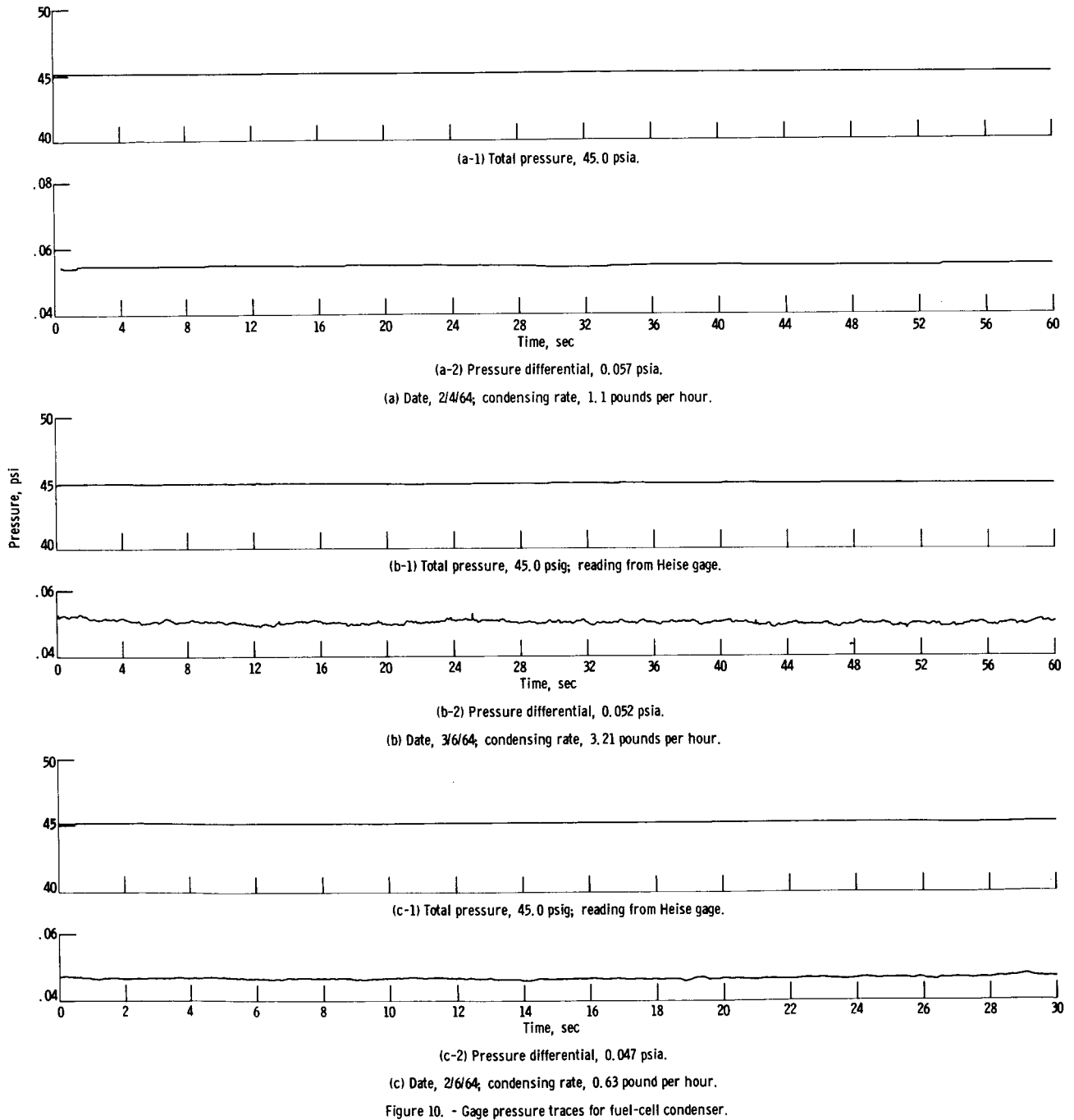


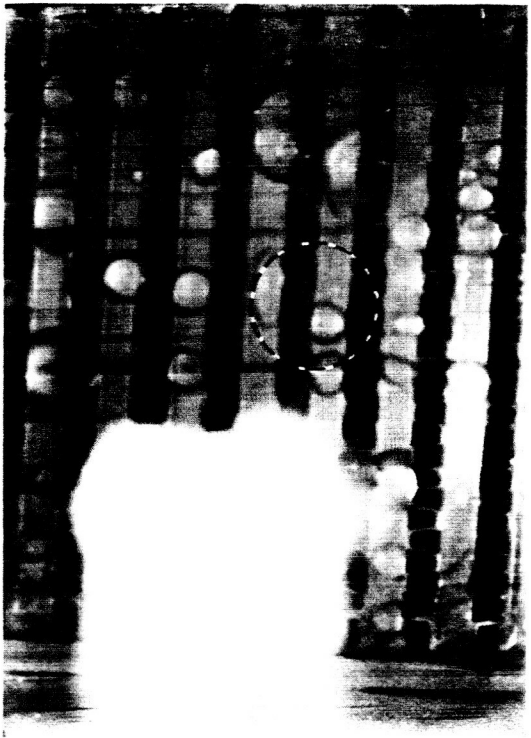
Figure 8. - Hydrogen plus water condenser assembly. (All dimensions in inches.)



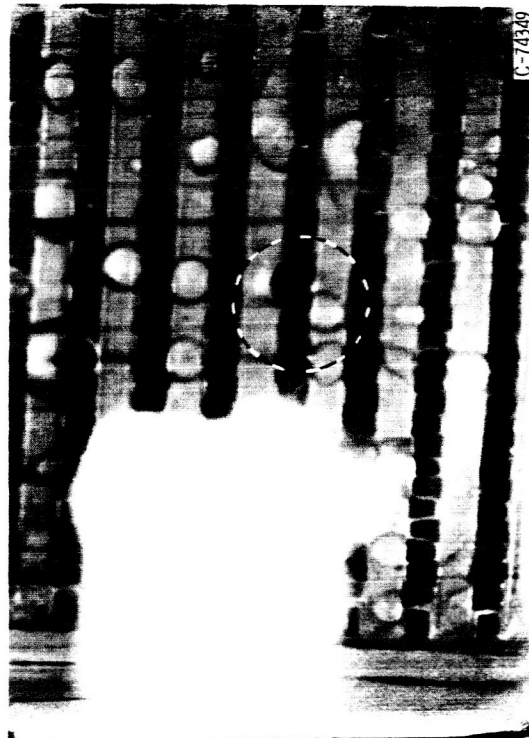
C-69693

Figure 9. - Flow control orifice.





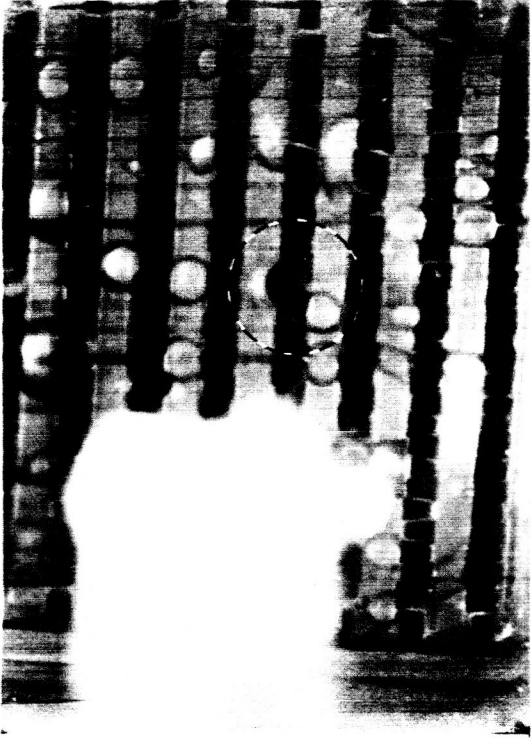
0 sec



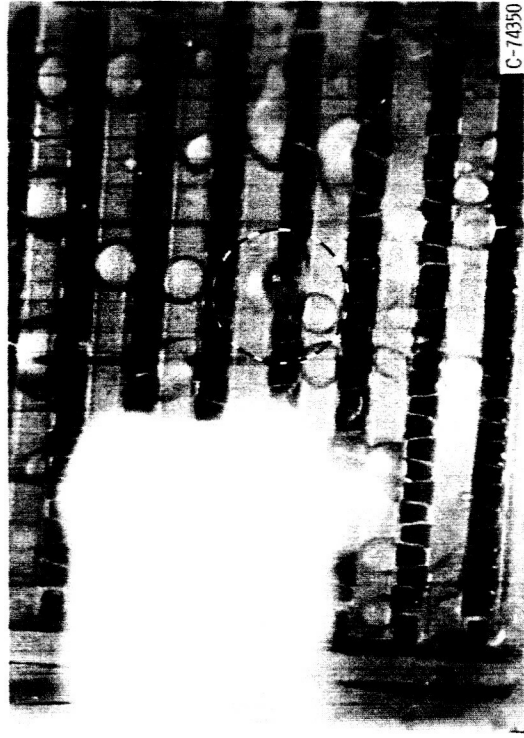
0.009 sec

C-74349

Figure 11. - Sequence of movie frames showing slug of condensate emerging from condensing tube.



0.018 sec



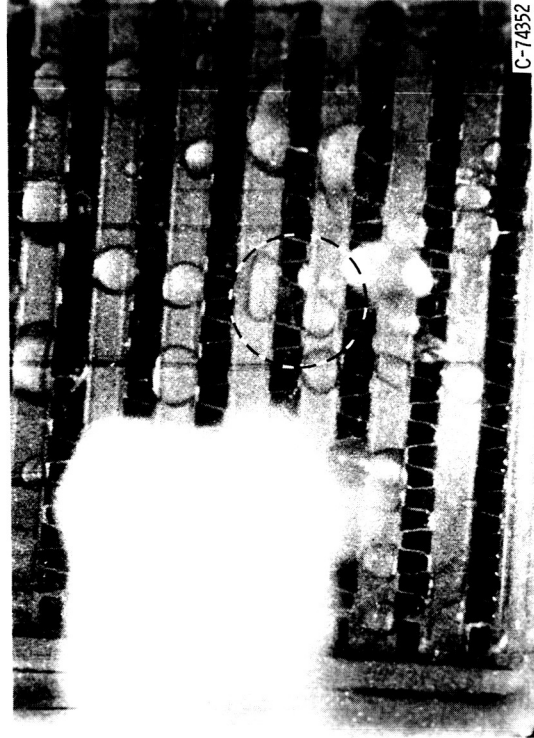
0.027 sec

C-74350

Figure 11. - Continued. Sequence of movie frames showing slug of condensate emerging from condensing tube.



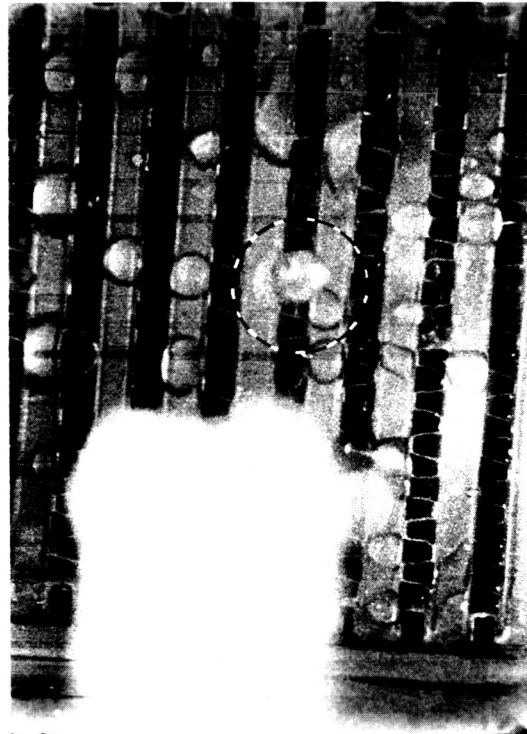
0.054 sec



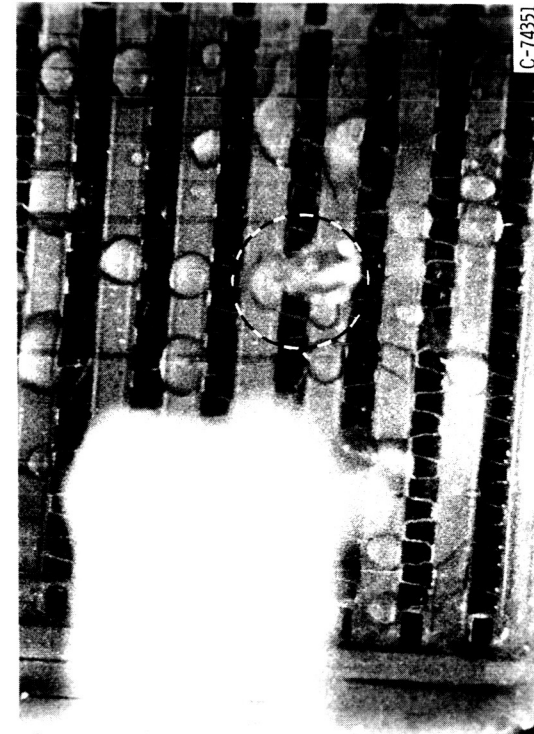
C-74352

0.063 sec

Figure 11. - Continued. Sequence of movie frames showing slug of condensate emerging from condensing tube.



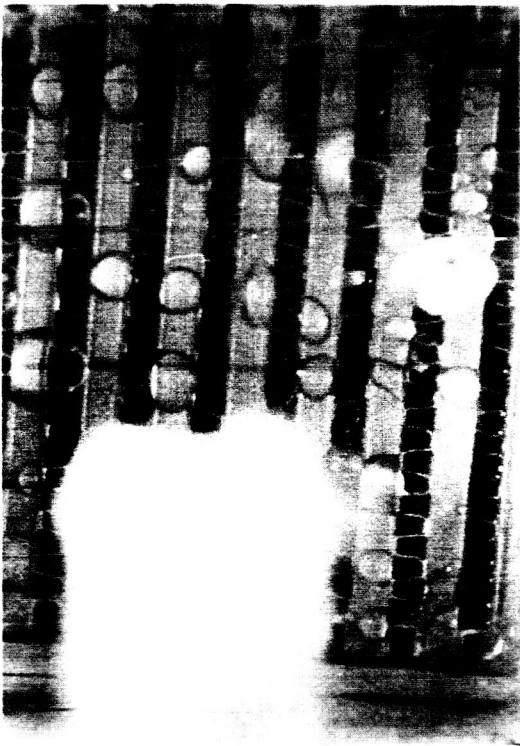
0.036 sec



C-74351

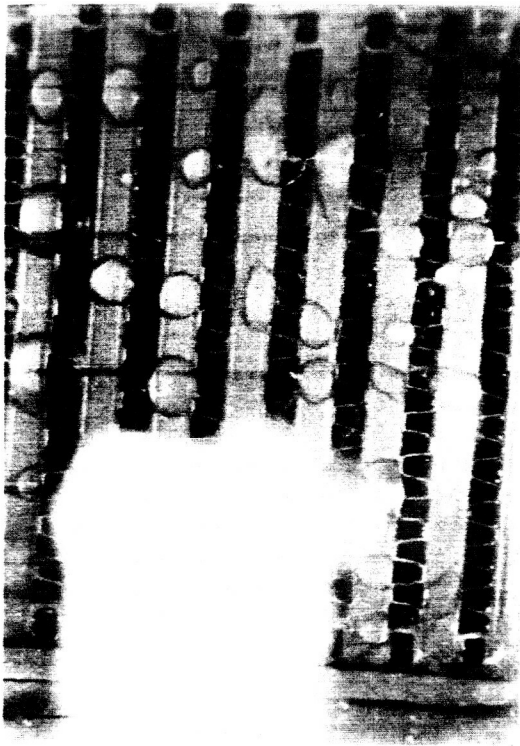
0.045 sec

Figure 11. - Continued. Sequence of movie frames showing slug of condensate emerging from condensing tube.



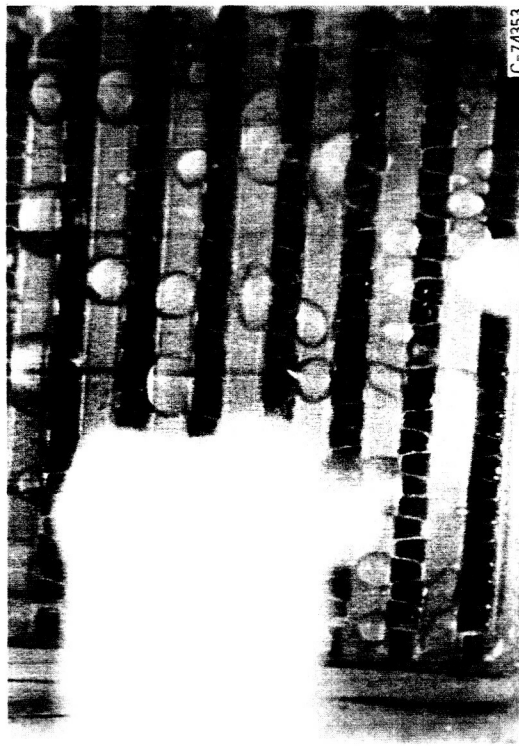
0.072 sec

C-74353



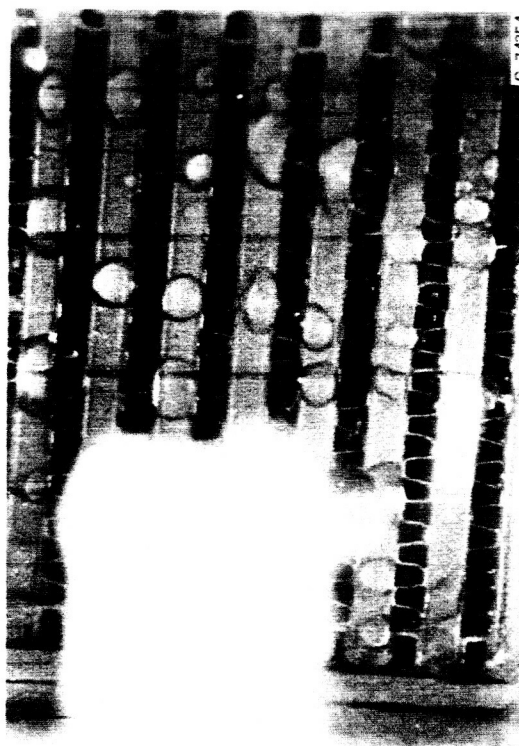
0.090 sec

C-74354



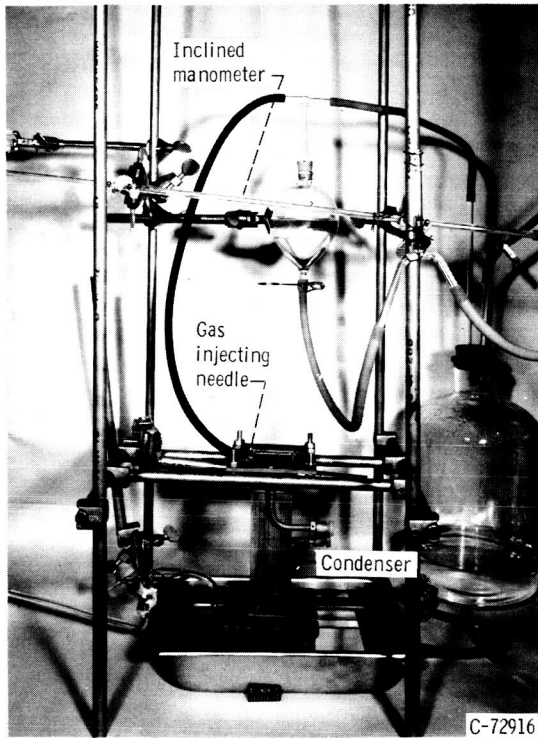
0.081 sec

Figure 11. - Continued. Sequence of movie frames showing slug of condensate emerging from condensing tube.

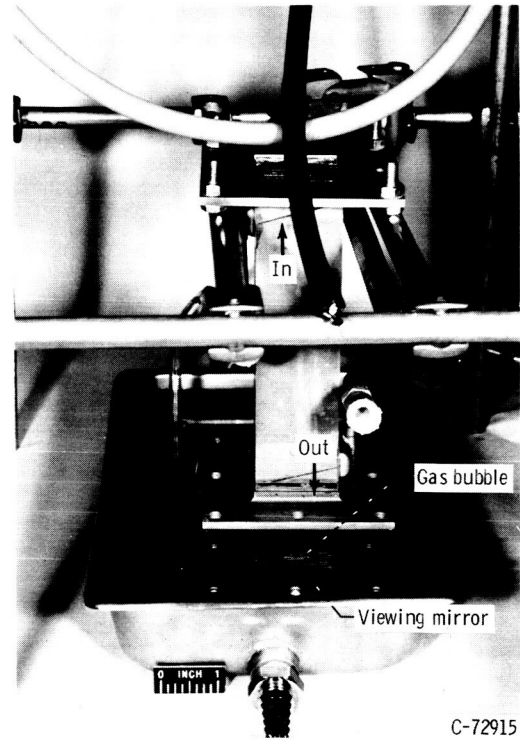


0.099 sec

Figure 11. - Concluded. Sequence of movie frames showing slug of condensate emerging from condensing tube.



(a) Overall view.



(b) Closeup view.

Figure 12. - Experimental determination of bubble pressure in condensing tubes.